Government of **Western Australia**
Department of **Mines and Petroleum**

RECORD 2012/12

HYPERSPECTRAL CHARACTERISATION OF RARE EARTH MINERALS

by
Sidy Morin Ka


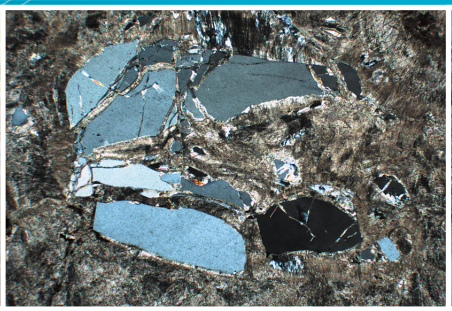


Geological Survey of Western Australia

Curtin University

Government of **Western Australia**
Department of **Mines and Petroleum**

Record 2012/12

HYPERSPECTRAL CHARACTERISATION OF RARE EARTH MINERALS

by
Sidy Morin Ka

Perth 2012

Geological Survey of Western Australia

MINISTER FOR MINES AND PETROLEUM
Hon. Norman Moore MLC

DIRECTOR GENERAL, DEPARTMENT OF MINES AND PETROLEUM
Richard Sellers

EXECUTIVE DIRECTOR, GEOLOGICAL SURVEY OF WESTERN AUSTRALIA
Rick Rogerson

Notice to the reader
This Record presents the results of studies as part of a Bachelor of Science Honours degree at Curtin University into hyperspectral characterisation of rare earth minerals. The Record has not undergone any editing by GSWA; only minor formatting. The views expressed in the Record do not necessarily reflect those of GSWA, but the Record is released to extend the level of understanding across a spectrum of disciplines in the region of exploring for rare earths by use of spectroscopic methods.

REFERENCE
The recommended reference for this publication is:
Morin Ka, S 2012, Hyperspectral characterisation of rare earth minerals: Geological Survey of Western Australia, Record 2012/12, 50p.

National Library of Australia Card Number and ISBN 978-1-74168-467-4

Grid references in this publication refer to the Geocentric Datum of Australia 1994 (GDA94). Locations mentioned in the text are referenced using Map Grid Australia (MGA) coordinates, Zone 50. All locations are quoted to at least the nearest 100 m.

Published 2012 by Geological Survey of Western Australia
This Record is published in digital format (PDF) and is available online at <http://www.dmp.wa.gov.au/GSWApublications>.

Further details of geological products and maps produced by the Geological Survey of Western Australia are available from:
Information Centre
Department of Mines and Petroleum
100 Plain Street
EAST PERTH WESTERN AUSTRALIA 6004
Telephone: +61 8 9222 3459 Facsimile: +61 8 9222 3444
www.dmp.wa.gov.au/GSWApublications

Geological Survey of Western Australia

Geological Survey of Western Australia

100 Plain Street | 6004 East Perth | Western Australia

In collaboration with

Curtin University

Faculty of Science and Engineering | Western Australian School of Mines

Department of Applied Geology

Kent Street | 6102 Bentley | Perth | Western Australia

Supervisors:

Dr. Lena Hancock - Geological Survey of Western Australia

Dr. Mehrooz Aspandiar - Curtin University

Abstract

The rare earth elements (REE) are a relatively abundant group of 15 elements composed of the lanthanides, plus yttrium. They are essential in many applications especially high technologies. Spectroscopy uses electromagnetic properties to identify and quantify the constitution of material. The HyLogging™ system is a reflectance spectroscopy tool for automated and quick logging of cores and samples used in geology. REE can be detected within minerals and drill cores using that system. Using known REE-bearing minerals from museum collection, a database has been created and characteristics defined. Then, those characteristics were applied to REE mineralisation in a drill hole containing REE from Cummins Range in Western Australia which had been assayed previously. The HyLogging™ system could be used to improve recognition and logging of the REE.

Acknowledgements

First, the author would like to thank Dr. Lena Hancock from the Geological Survey for her guidance and help throughout the project.

The author thanks the Geological Survey of Western Australia, especially Dr. Paul Morris and Mr. Don Flint for their support on this project.

Moreover, part of this project would not have been possible without the loan of rare-earth minerals form the Western Australia Museum and constructive talks with Dr. Peter Downes.

The author also thanks Mr. Michael Verrall, Manager of Electron Beam & XRD laboratories from the CSIRO, for the use and help with the SEM+EDAX device.

Last, thanks to Dr. Mehrooz Aspandiar for the introduction into this project and his wise advice.

Table of Contents

List of Figures

List of Tables

1. Introduction

The growing use and demand for rare earth elements (REE) due to their increase use in modern technologies, the limited supply of these commodities and the market dominance of China leading to strategic concerns in other nations, make the REE a strategic resource.

High technology and environmental applications of the REE have grown considerably in diversity and importance over the past four decades. As many of these applications are highly specific, in that substitutes for the REE are inferior or unknown, the REE have acquired a level of technological significance much greater than expected from their relative obscurity. Although actually more abundant than many familiar industrial metals, the REE have much less tendency to become concentrated in exploitable ore deposits. Consequently, most of the world's supply comes from only a few sources, with China producing over 90% of the market (Chen, 2011; Kanazawa and Kamitani, 2006; U.S. Geological Survey, 2011).

Global demand for rare earth resources is experiencing extremely fast growth. Mine production is decades behind projected short-term needs. China's policy initiatives restrict the exports of processed rare earth raw materials, especially the heavy rare earths (HREE). China wants an expanded and fully integrated REE industry where exports of value-added REE-bearing materials are preferred. China wants to build strategic stockpiles of raw materials as South Korea and Japan have done, and thus have even stronger control over global supply and prices (Humphries, 2010).

With this background behind the REE, Australia has its part to play as it possesses one of the biggest deposits known (i.e., Mt Weld, Western Australia) and several others deposits. In addition, Australia possesses a technology via the CSIRO called the HyLogging™ system, which might prove to be reliable as a REE exploration and research tool.

This project focuses on hyperspectral characteristics of the rare earths using the HyLogging system with REE minerals from the Western Australia Museum and a drill hole from a regolith-carbonatite-hosted REE deposit at Cummins Range, Western Australia.

2. What are the REE?

The rare earths (Table 1) are the group of 15 elements named the lanthanides; additionally yttrium and scandium are commonly included with these elements because they share chemical and physical similarities. The term Rare Earth Elements (REE) is misleading as they are relatively abundant in the earth's crust. For instance cerium is the 25th most abundant element of the 78 common elements in the earth's crust at 83 parts per million (U.S. Geological Survey, 2011) and mercury averages lower than thulium which is the rarest among the REE (Dill, 2010).

The REE are divided in two types: on the one hand, the light rare earth elements (LREE) tend to occupy larger lattice with 8–10 coordination numbers and concentrate in carbonates and phosphates. On the other hand, heavy rare earth elements (HREE) and Y occupy 6–8 coordination number sites and are abundant in oxides and some phosphates (Dill, 2010).

Table 1 Rare Earths classified by atomic number with their atomic weight, symbol and average grade (modified from Dill, 2010)

Element	Atomic No.	Symbol	Atomic Weight	Average grade (earth crust)	
Lanthanum	57	La	138.92	50 ppm	**Light Rare Earth elements (LREE)**
Cerium	58	Ce	140.13	83 ppm	
Praseodymium	59	Pr	140.92	13 ppm	
Neodymium	60	Nd	144.27	44 ppm	
Promethium*	61	Pm	145.00	NA	
Samarium	62	Sm	150.43	7.7 ppm	
Europium	63	Eu	152.00	2.2 ppm	
Gadolinium	64	Gd	156.90	6.3 ppm	**Heavy Rare Earth Elements (HREE)**
Terbium	65	Tb	159.20	1.0 ppm	
Dysprosium	66	Dy	162.46	8.5 ppm	
Holmium	67	Ho	163.50	1.6 ppm	
Erbium	68	Er	167.20	3.6 ppm	
Thulium	69	Tm	169.40	0.5 ppm	
Ytterbium	70	Yb	173.04	3.4 ppm	
Lutetium	71	Lu	174.99	0.8 ppm	
Yttrium[1]	39	Y	45.10		

*Promethium does not occur naturally as a stable isotope, although it can be artificially manufactured

[1]Yttrium is considered a REE because it shares chemical similarities and occurs with the HREE

The REE share many common physical and chemical properties that make them difficult to distinguish from each other or chemically separate (Hoatson et al., 2011). Such common properties include:

- silver, silvery-white, and grey metallic colours; soft, malleable, and ductile behaviours
- high lustres, which readily tarnish in air; high electrical conductivities
- reactive states (to form REO) especially at high temperatures
- very small differences in solubility and complex formation between the REE
- dominant oxidation valence state of +3 when the REE are associated with non-metals (although europium has a valence state of +2 and cerium +4)

2.1. Where are they found?

Rare-earth elements do not occur as free metals in the Earth's crust, such that all naturally occurring minerals consist of mixtures of various REE and non-metals. Bastnäsite [(Ce,La)(CO_3)F], monazite [(Ce,La,Nd,Th) PO_4], and xenotime (YPO_4) are the three most economically significant minerals of the 200 plus minerals known to contain essential or significant REE (Christie et al., 1998).

Bastnäsite and monazite are is the principal sources of LREE, which accounting for about 95% of the REE utilised (Cooper, 1990) whereas xenotime is the principal sources for HREE.

2.2. Geological environment of REE mineralization

Bastnäsite occurs predominantly in calc-silicate rich rocks related to alkaline intrusive igneous complexes, in particular carbonatite, dolomitic breccia with syenite intrusives, pegmatite, and amphibolite skarn. Monazite and xenotime are more common as accessory minerals in low-calcium granitic rocks, gneisses, pegmatites, and aplites. Xenotime is commonly associated with zircon and can enclose that mineral. Following weathering of granites and pegmatites, monazite and xenotime are concentrated in heavy mineral placer deposits because of their resistance to chemical attack and high specific gravities. Other commercial sources of REE are apatite and loparite (western Russia), REE-bearing clays ('Longnan clay' or 'southern ionic clay', Jiangxi Province, China), and various minerals, such as allanite that are produced as a by-product of uranium mining (Canada). Of lesser importance are zircon containing (Th, Y, and Ce) and euxenite.

2.3. REE bearing minerals

Bastnäsite $(Ce)_2(Ce,La)(CO_3)F$ is a fluoro-carbonate of cerium metals containing 60 to 70% REO including lanthanum and neodymium. Monazite $(Ce,La,Nd,Th)PO_4$ is a cerium, lanthanum and neodymium-bearing phosphate containing 50 to 78% REO. Monazite is also the principal ore of thorium, containing up to 30% thorium, which together with smaller quantities of uranium (up to 1%) imparts radioactive properties to the monazite. Xenotime is an yttrium-bearing phosphate hosting 54 to 65% REO, and comprising other REE such as erbium and cerium, and thorium. Xenotime (YPO_4) (Table 2) and minerals such as allanite $(Ce,Ca,Y)_2(Al,Fe)_3(SiO_4)_3(OH)$ are common sources of the HREE and yttrium (Hoatson et al., 2011). The major REE-bearing minerals are compiled in table 2.

Table 2 Rare-earth element bearing minerals (major and common) (modified from Hoatson et al., 2011)

Mineral	Mineral chemistry	wt% REO
Allanite (orthite)	$(Ce,Ca,Y)_2(Al,Fe)_3(SiO_4)_3(OH)$	3 to 51
Apatite	$Ca_5(PO_4,CO_3)_3(F,Cl,OH)$	19
Bastnäsite–(Ce)	$(Ce)_2(Ce,La)(CO_3)F$	70 to 74
Monazite–(Ce)	$(Ce,La,Nd,Th)PO_4$	35 to 71
Parisite	$Ca(Ce,La)_2(CO_3)_3F_2$	59
Xenotime–(Y)	YPO_4	52 to 67

Apatite is not a great REE bearer but it may become a major REE source in certain mineralisation due to its high abundance. Many other rarer minerals also bear REE [e.g., loparite $(Ce,Na,Ca)(Ti,Nb)O_3$, synchysite $(Ca(Ce,La)(CO_3)_2F]$. Currently over 200 REE-minerals are known.

3. Spectroscopy and the HyLogging™ system

3.1. Principle

3.1.1. Electromagnetic radiation

Electromagnetic radiation is composed of oscillating electric and magnetic fields that have the ability to transfer energy through space. The energy propagates as a wave, such that the crests and troughs of the wave move in vacuum at the speed of light (299,792,458 m/s). The many forms of electromagnetic radiation appear different to an observer; light is visible to the human eye, while X rays and radio waves are not (Encyclopædia Britannica, 2011).

The distance between successive crests in a wave is called its wavelength. The various forms of electromagnetic radiation differ in wavelength. For example, the visible portion of the electromagnetic spectrum lies between 4×10^{-7} and 8×10^{-7} metre (400 to 800 nanometre (nm)) (Encyclopædia Britannica, 2011).

3.1.2. Absorption spectroscopy

Absorption spectroscopy measures the loss of electromagnetic energy after it illuminates the sample under study. For example, if a light source with a broad band of wavelengths is directed at a vapour of atoms, ions, or molecules, the particles will absorb those wavelengths that can excite them from one quantum state to another. As a result, the absorbed wavelengths will be missing from the original light spectrum after it has passed through the sample. Since most atoms and many molecules have unique and identifiable energy levels, a measurement of the missing absorption lines allows identification of the absorbing species. Absorption within a continuous band of wavelengths is also possible. This is particularly common when there is a high density of absorption lines that have been broadened by strong perturbations by surrounding atoms (e.g., the effects of near neighbours) (Encyclopædia Britannica, 2011).

There are two general processes causing absorption spectral features – electronic and vibrational (such as crystal field effects, charge transfer, colour centres, conduction bands) and symmetric/asymmetric stretches and bendings (Clark, 1999).

3.2. Application

The reflectance spectroscopy is one of the analytical techniques coming from the spectroscopy principle.

Production and analysis of a spectrum require a source of light (or other electromagnetic radiation), and a detector to sense the presence of light after reflection. The device used to accept light, separate it into its component wavelengths, and detect the spectrum is called a spectrometer. Spectra are obtained in the form of reflectance spectra, which show absorption features within the returning spectra.

The HyLogging system is a geologic tool using this method.

3.3. HyLogging™ system

The HyLogging system permits non-destructive and non-contact scanning of drill cores, chips or hand samples. One restriction to the method is that it requires dry and clean samples.

The HyLogging hardware system comprises an integrated suite of spectroscopic, imaging, lighting, and materials handling tools that enable core to be scanned semi-automatically. The HyLogging hardware is complemented by The Spectral Geologist (TSG) software for the analysis, mineralogical interpretation, and simultaneous visualization of the spectral, image, and mineralogical data (Hancock and Huntington, 2010a).

Currently, the HyLogging scanning involves measuring scattered (reflected and transmitted) light from the sample surface, within the wavelength range of visible to near-infrared (VNIR; 380–1000 nm), shortwave-infrared (SWIR; 1000–2500 nm), and thermal infrared range (TIR; 6000–14 000 nm) in the electromagnetic spectrum (Table 3) (Hancock and Huntington, 2010b).

Table 3 Minerals detected at different wavelengths (Hancock and Huntington, 2010b)

Wavelength region	Wavelength range (nm)	Mineralogy
VNIR	400-1100	Iron oxides and hydroxides, rare earths
SWIR	1100-2500	Hydroxyls (aluminium, magnesium and iron), carbonates,
TIR	6000-14 000	Carbonates and silicates; including quartz, feldspar, plagioclase,

3.3.1. HyLogger™

The HyLogger (Figure 1) is the name given to the hardware part of the HyLogging system. It scans cores and samples using a computer-controlled table that continuously moves the core in a zigzag path beneath the scanner at a rate of approximately one metre every 30 seconds. Spectrometers measure radiance, which is converted to spectral reflectance in relation to a "Spectralon" standard. The spectrometer instantaneous-field-of-view is 8 mm in diameter. The imaging system is a digital three-colour (red, green, blue) area-array camera used in a line-scan mode with a resolution of 0.1 mm (Hancock and Huntington, 2010a).

The system constructs a continuous image of the core, frame by frame, as the tray passes underneath. The system incorporates a laser "profilometer" used to measure the physical condition of the core every 0.1 mm as well as fractures and breaks to assist in geotechnical assessment and for control of other aspects of the system. The spectrometer, image, and "profilometer" data are captured simultaneously during a single traverse of the core tray (Hancock and Huntington, 2010a).

The HyLogger accepts drillcore of any diameter, presented in standard core trays. The core must be dry and clean.

Figure 1 Picture of a HyLogger™: an integrated suite of spectroscopic, imaging, lighting, and materials handling tools (Hancock and Huntington, 2010a)

3.3.2. *The Spectral Geologist™ (TSG)*

The TSG software (Core version) is used for the spectral analysis, mineralogical interpretation, and interactive visualization of spectral, image, and mineralogical data, plus the creation of output products. It supports the HyLogger and can recognize about 60 minerals including iron oxides, phyllosilicates, hydroxylated silicates, sulfates, carbonates, and ammonium-bearing minerals. The new TIR spectrometer expands the spectral range of the HyLogger (104 minerals in the TIR library) , allowing a wider variety of anhydrous mineral species (e.g. feldspars, pyroxenes, olivines, garnets, and quartz), including framework silicates and orthosilicates, to be sensed (Table 3) (Hancock and Huntington, 2010b). The reference set of scanned minerals is continuously being expanded as a result of scanning by others around the world but particularly by those using the CSIRO HyLoggers in Australia

3.3.3. *Methodology*

The HyLogger owned by the Geological Survey of Western Australia was used to scan the Cummins Range drill hole. It took two days to scan the 54 trays for a total of 402 metres.

The HyLogger needs to be calibrated and set up before use. To do so the steps used are described in the following paragraph.

The HyLogger was filled with liquid nitrogen for cooling down SWIR and TIR detectors and left for 15 minutes before calibration.

- Calibration:
  - Temperature calibration for TIR spectrometer with a cold and hot target
  - White and black body calibration for SWIR and TIR spectrometers test rocks (i.e., a set of different rocks that have known spectra and are used as reference)
- Scanning:
  - Temperature in the room should be constant and checked regularly
  - The trays must be at the same temperature as the room, therefore they are left for 15 minutes inside the room before scanning. This is important for TIR measurement
  - Interfered light must be avoided and low light emission must be kept
  - The white reference is redone once a day
  - The drill cores are placed optimally and dusted off if necessary

4. REE spectra database creation

REE bearing minerals (i.e., monazite, bastnasite, parisite, xenotime) were lent to the author by the Western Australia Museum in order to create a reference set to include in the TSG database of minerals. In addition, by creating that reference set it enables the comparison of these REE bearing minerals with the Cummins Range drill core.

4.1. Minerals

Twenty-one minerals (Appendix 1–5) from worldwide locations were used to create the database; they are reported in Table 4.

Table 4 REE minerals used to create the database of REE signature

Mineral	Number of samples	Results	HyLogger pictures
allanite	***1***	No signature, too dark to reflect enough light to the spectrometer	
apatite	***7***	4 with REE signature 1 with a low REE signature 2 with no signature	
bastnasite	***1***	Good signature for REE	
monazite	***8***	7 with REE signature 1 was actually a xenotime	
parisite	***1***	Good signature for REE	
xenotime	***3***	Signature for Y and HREE	

4.2. Methodology

The samples are separated by type; no particular preparation is needed excepting cleaning away the dust. They were placed on a black cover to avoid any interference due to non-desired reflected light, then scanned with the HyLogger using the same methodology described in section 3.3.3.

4.3. Spectrometric characteristics

According to Clark, R.N. (1999) the absorption bands due to rare earth elements are not diagnostic of mineralogy but of the presence of the ions in the mineral. These absorptions are due to crystal-field transitions involving deep-laying electrons of the rare earth element and do not shift when the rare-earth ion is in another mineral.

REE give a signature composed of sharp features (e.g., 802nm) as shown in Figure 2. That signature is composed of features present from the VNIR to the SWIR, but no REE features are present in the TIR.

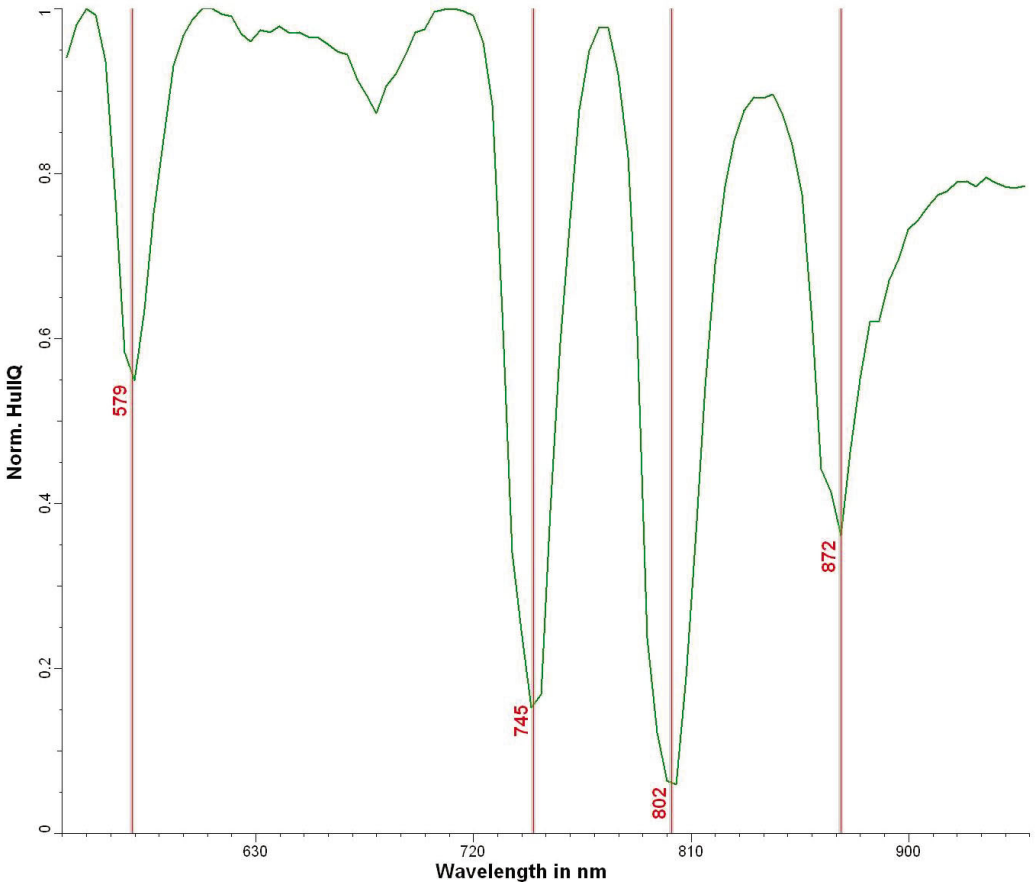

Figure 2 Visible signature of REE. It is composed of four major features at 579, 745, 802 and 872 nanometre.

However, a slight shift can be noticed between phosphate and carbonate minerals. Phosphate minerals have all their features shifting to longer wavelengths (by about ± 4 nm). That shifting could be used to distinguish the type of REE bearing mineral.

Moreover, xenotime gives different features as seen in Figure 3. Therefore, no doubt can be done with the other minerals. It appeared that the monazite MDC2323 gave a xenotime signature, moreover the apatite S2159 had no REE signature.

4.3.1. REE signature and main features

Bastnasite and parisite (carbonate minerals) have their main features at 579/742/800/868 nm, when monazite and apatite (phosphate minerals) have their main features at 581/746/803/872 nm and apatite features are similar when present (Appendix 6). Xenotime has its main feature 668/809/915/1137 nm Table 5.

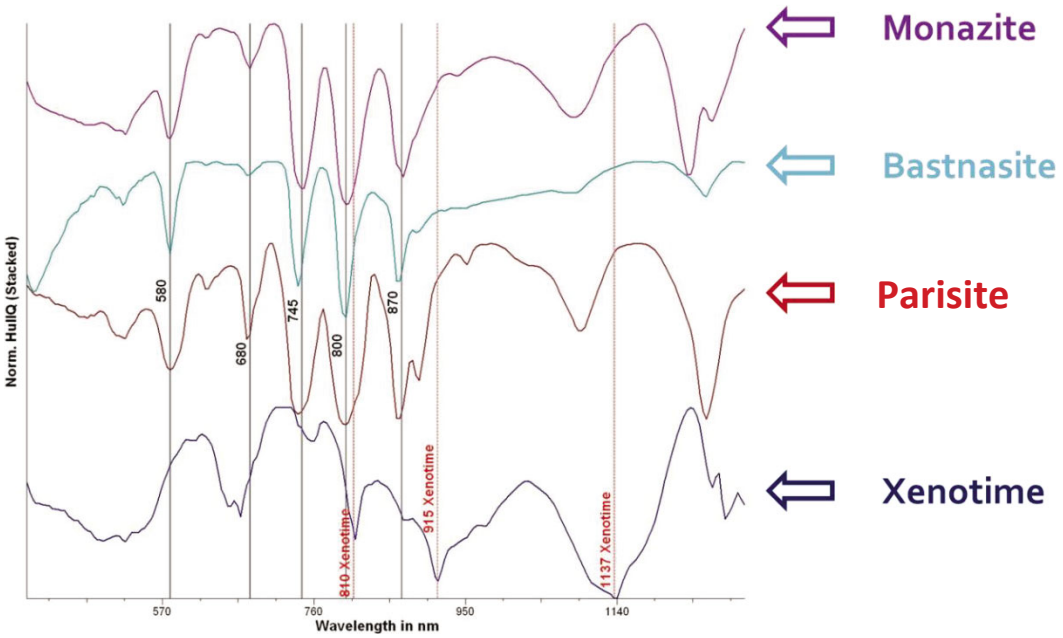

Figure 3 REE signatures for the major minerals (each line corresponds to an absorption feature)

Features found for xenotime are interpreted as being the contribution of Yttrium and HREE in place of LREE for the other minerals.

Absorption features from the museum minerals combined with features from REE oxides from Rowan et al (1986) and Weidner et al (1986), are compiled in the table 5. Data from Rowan et al (1986) and Weidner et al (1986) helped to distinguish features related to rare earth elements from those associated with the REE bearing mineral.

Table 5 Absorption features of REE minerals and REE-oxides (REE oxides from: Rowan et al., 1986; Weidner et al., 1986)

	VISIBLE →														SWIR
Mineral	**Absorption features in nanometre (nm)**														
Monazite				581			680	745	802	872				1090	
Apatite	415			582				747	805	873					
Bastnasite	415			578			680	742	800	868	892			1086	
Parisite				580			680	740	800	868	892			1094	
Xenotime	412				652	668			809			915			1137
REE oxides															
LREE															
[1] Pr_2O_3				590						850		910			
[1] Nd_2O_3	420	475	525	580			680	740	800	870					
[1] Sm_2O_3	410	470											960	1090	
HREE															
[1] Eu_2O_3		470	530												
[2] Dy_2O_3								743	799	886		907		1065	1096
[2] Ho_2O_3															1132 1149
[2] Er_2O_3													972 981 1013		

KEY: Non reliable | Doublet | Main features | Features | Weak

[1] REE oxides results from Weidner et al.(1986)

[2] REE oxides results from Rowan et al.(1986)

Full table with VNIR and SWIR features available as Appendix 14

4.4. Scanning Electron Microscope with Energy-Dispersive X-ray Spectroscopy

In order to confirm the results found by the HyLogger® and to be sure of the presence of REE, the samples were also tested via the Scanning Electron Microscope (SEM) fitted with an Energy Dispersive x-ray Spectrometer (EDS).

The SEM (as seen in Figure 4) is an instrument that produces a highly magnified image by using electrons instead of light to form an image. A beam of electrons is produced at the top of the microscope by an electron gun. The electron beam follows a vertical path through the microscope. The beam travels through electromagnetic fields and lenses, which focus the beam down towards the sample. Once the beam hits the sample, electrons and X-rays are ejected from the sample (Schweitzer, 2011).

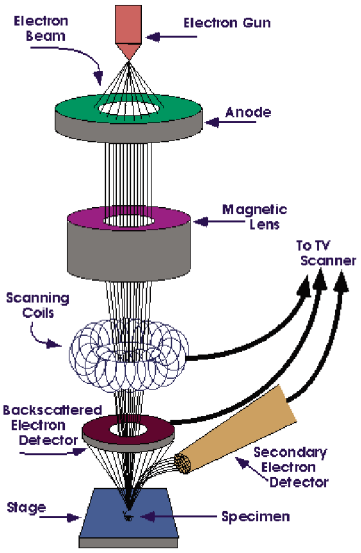

Figure 4 Diagram of an SEM (Schweitzer, 2011)

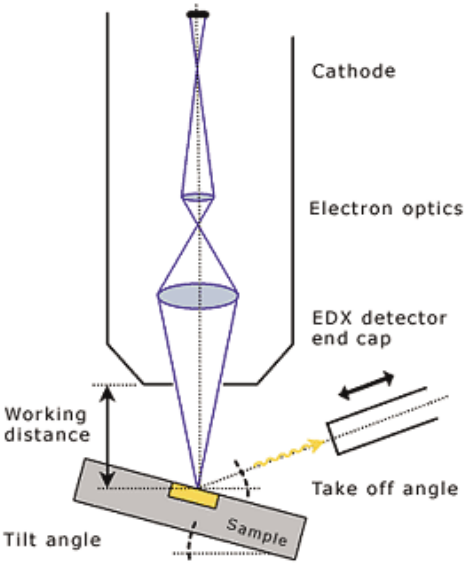

Figure 5 Diagram of the EDS (Bruker, 2011)

The EDS system (Figure 5) exploits the interaction between high-energy electrons and a sample under investigation in an electron microscope, the atoms of this sample are caused to emit X-rays. The system makes use of the fact that atoms of different chemical elements emit X-rays of different, characteristic energy. The evaluation of the energy spectrum collected by the X-ray detector allows the determination of the qualitative and quantitative chemical sample composition at the current beam position. One advantage of the energy dispersive X-ray spectroscopy is that all elements from atomic number 4 (beryllium) up to 95 (americium) contained in the sample can be detected and analysed

simultaneously (Bruker, 2011).When used with scanning microscopes (SEM), the EDS system can analyse element distributions along a line (line scan) or within an area of interest (mapping) with a spatial resolution in the nanometre range.

4.4.1. Methodology

The data was collected on a Philips (FEI) XL40 controlled pressure SEM fitted with an EDAX energy dispersive x-ray spectrometer. The system was operated with an accelerating voltage of 30kV and a chamber pressure of 0.5mBar. The samples were examined uncoated and all the images were collected with a Robinson back scattered electron detector.

4.4.2. Results

Observation of the samples with the SEM showed that the minerals were mixture of REE-rich patches scattered within a phosphate/carbonate matrix (Figure 6 and Table 7). The SEM was used to locate the spots to analyse with the EDAX.

The EDAX results (Appendix 7–11) confirmed that the minerals scanned contained REE and therefore that the signature observed were related to them.

Monazite MDC 2323 is confirmed to be a xenotime as yttrium is the major element and it is relatively rich in HREE (Table 6).

Oxide	Wt %
P_2O_5	27.93
PbO	0.24
ThO_2	2.46
UO_2	3.11
Sm_2O_3	1.6
EuO_2O_3	0.43
Gd_2O_3	**4.16**
Tb_2O_3	**1.61**
Dy_2O_3	**7.4**
Ho_2O_3	**1.09**
Er_2O_3	**1.67**
Tm_2O_3	**0.25**
Yb_2O_3	**0.92**
Y_2O_3	**47.12**
Total	**100**

Table 6 EDAX results for xenotime MDC 2323. Green colour corresponds to REE oxides

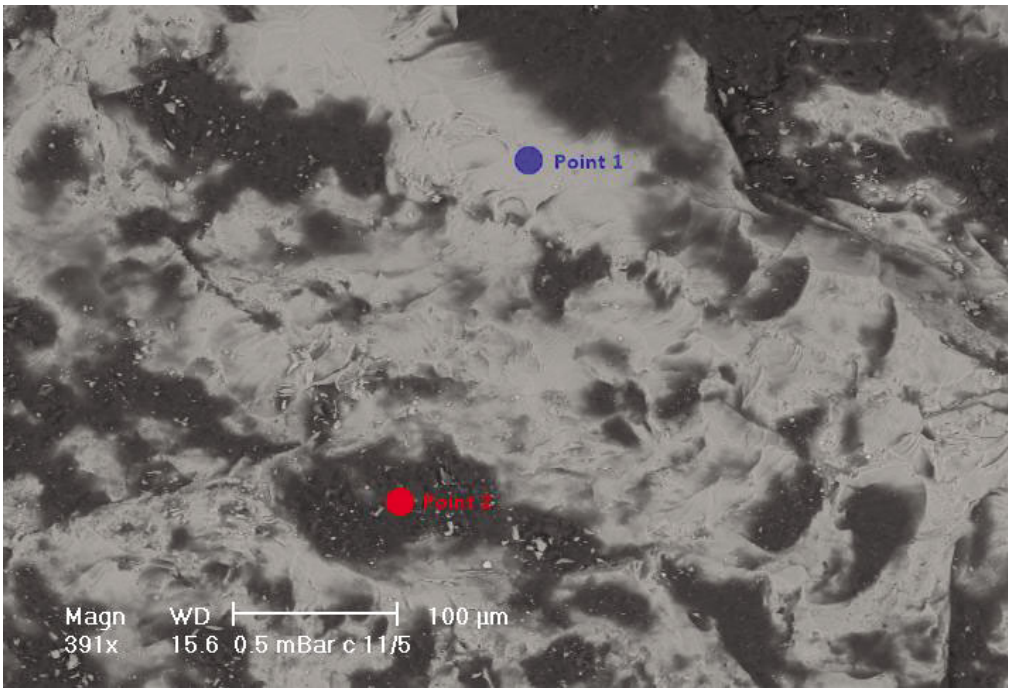

Pilganoora (N.W.) 6 miles north Western Australia

Figure 6 Sample of monazite MDC 1276: Hand specimen SEM image, with analysis

Table 7 EDAX results for monazite MDC1276 on two different points. Green colour corresponds to REE oxides

Point 1		Point 2	
Oxide	**Wt %**	**Oxide**	**Wt %**
Al_2O_3	3.34	Al_2O_3	35.78
SiO_2	5.98	SiO_2	50.35
P_2O_5	28.18	K_2O	1.5
ThO_2	2.2	TiO_2	1.1
CaO	0.02	FeO	11.27
La_2O_3	**5.57**	***Total***	***100***
Ce_2O_3	**23.97**		
Pr_2O_3	**3.97**		
Nd_2O_3	**14.7**		
Sm_2O_3	**7.44**		
Gd_2O_3	**4.64**		
Total	***100***		

5. Application to Cummins Range

The Cummins Range deposit (Table 8) is a REE-bearing laterite associated with carbonatite complex located in Western Australia (Hoatson et al., 2011). Cummins Range is still on the exploration stage with ongoing exploration by Kimberley Rare Earths Ltd.

Table 8 Cummins Range (data from Hoatson et al., 2011; U.S. Geological Survey, 2011)

Deposits	**Cummins Range**
Country	Australia
State	West Australia
Geographic location	Halls Creek, Kimberley
Age	1012 million years
Ore body form	plug
Ore body length	1.8km
Ore body width	1.7km
Ore body area	2.4 km^2
Alteration type	Amphibolization, carbonatization
Resource tonnage	4.2 million tonnes
REE grade	1.7%

The Geological Survey of Western Australia is in possession of one drill hole (i.e., CDD1) from the 1984 drilling campaign by CRA Exploration Pty Ltd. This drill hole goes through the REE mineralisation as reported by Richards, (1985). This is why this drill hole had been used and compared to the REE database created as explained in Section 4. Signatures from REE are expected and results will show if the HyLogger can detect these.

5.1. Location

The Cummins Range deposit is located 130Km SSE of Halls Creek in Western Australia (Figure 7). The carbonatite is located at the junction of the Halls Creek and King Leopold mobile zones on the southern margin of the Kimberley craton. It is a vertical pipe-like body, which intrudes Proterozoic metasediments and granite gneiss (Richards, 1985). It has been interpreted to be emplaced in the proximity of the Halls Creek Fault (Sweetapple and Downes, 2010). Country rocks, including granite gneiss and chlorite schist, are interpreted to be part of the Eastern zone of the Palaeoproterozoic Lamboo Complex (Andrew, 1990).

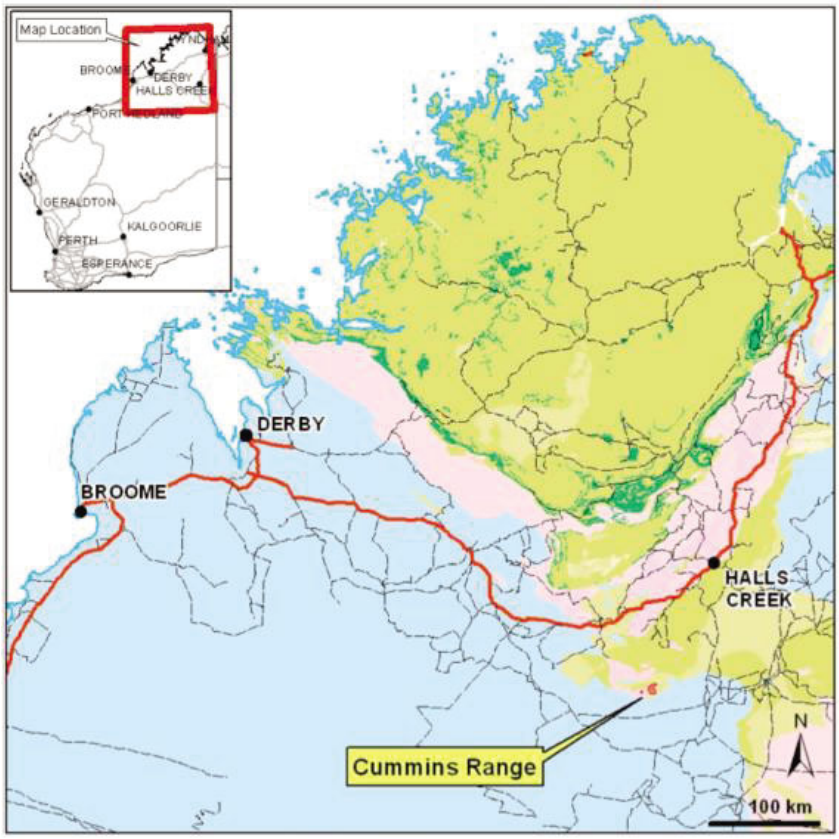

Figure 7 Location of Cummins Range, South Kimberley, Western Australia (Kimberley Rare Earths, 2011)

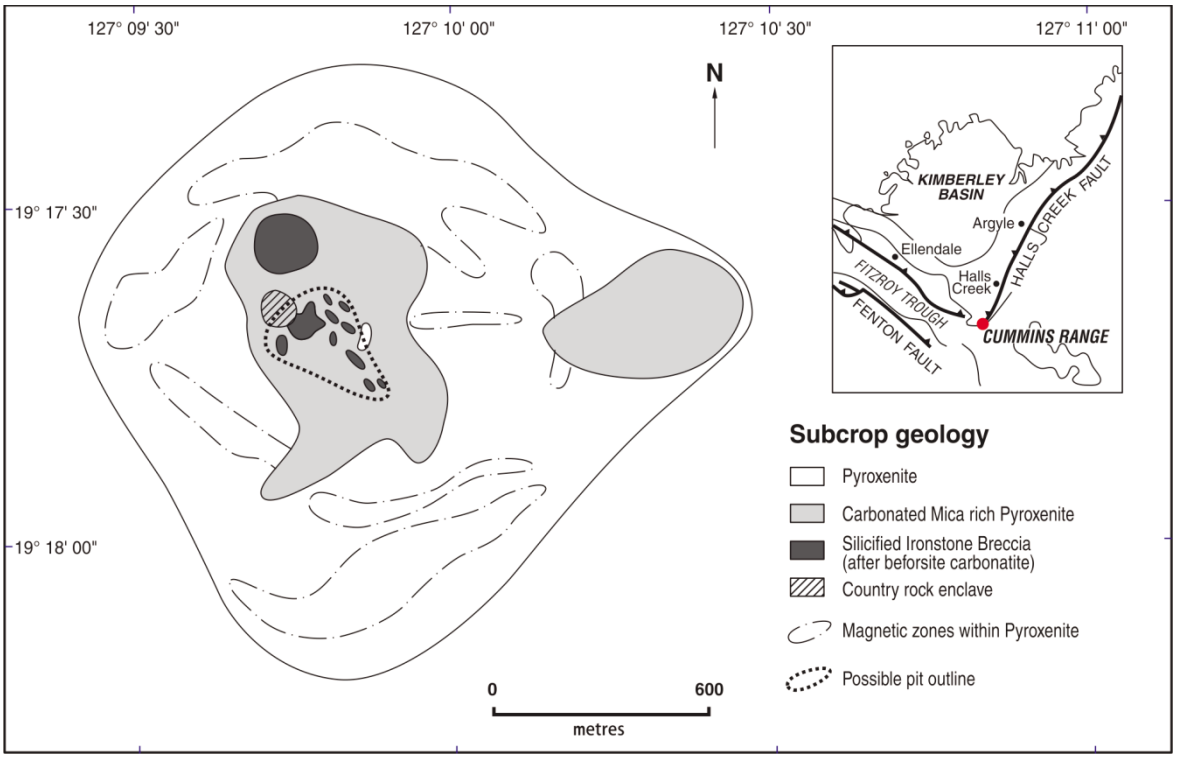

Figure 8 Subcrop geological plan of Cummins Range carbonatite and associated intrusive complex (Andrew, 1990)

5.2. Geology

The carbonatite lies at the southern apex of the Kimberley block at the junction of the Halls Creek and King Leopold mobile zones (Figure 8). The Halls Creek Province containing these mobile zones is an important alkaline igneous province, the carbonatite complex intrudes a sequence of slate, phyllite and metagreywacke, correlated with those of the Proterozoic Olympio Formation of the Halls Creek Group (Yeates and Muhling, 1977). Granite gneiss also forms part of the country rock, and probably belongs to the Lamboo Complex (Andrew, 1990). The intrusive is of late Proterozoic age and may be related to the coeval Bow Hill lamprophyre dyke swarm in the East Kimberley (Fielding and Jaques, 1986).

The Cummins Range complex is a 1.7Km by 1.8Km vertical pipe-like body (Figure 8) of pyroxenite that has been intruded and altered by a number of vertical to sub-vertical carbonatite dykes. The intrusion of the carbonatite dykes and the resultant alteration has produced three main concentric zones. An outer unaltered pyroxenite zone, an inner carbonated micaceaous amphibolite zone and a central carbonatite zone (Figure 8).

The intrusion of the volatile-rich carbonatite dykes has variously metasomatised or fenitized the surrounding host pyroxenite. The metasomatism increases towards the central carbonatite plug, resulting in the zonation (Richards, 1985).

The rare earths, niobium and apatite mineralization is a feature of the weathered zone produced by the physical concentration of resistant minerals under strong dissolution, leaching and weathering conditions. Weathering of the complex is deep and typical of a moist tropical climate. This style of weathering is most pronounced in the carbonatite rocks where processes typical of karst environments, such as dissolution, leaching and collapse brecciation, have produced jasperoidal ironstone breccias. Within the oxidized zone, leaching and dissolution of the carbonates and weathering of the silicates have physically concentrated resistate minerals such as monazite, apatite and pyrochlore to levels often greater than ten times the concentrations within the primary rocks. This mineralization is best developed in the central portion of the complex where the density of carbonatite dykes is the greatest and the weathering is the most intense.

The process of weathering has been the major factor in upgrading the mineralization at Cummins Range. REE–Nb–Ap decrease in concentration radically below the weathered zone (modified from Andrew, 1990; Richards, 1985).

5.3. Mineralogy

The carbonatite rocks are composed of more than 90% carbonate. In most cases, the carbonate is dolomite (beforsite). Calcite (sovite) and magnesite-carbonate species are also present. Minor and accessory minerals include: amphibole, biotite, magnetite, chlorite, apatite, monazite, zircon, bastnäsite, aeschynite, fluorite, pyrochlore, allanite, pyrrhotite, pyrite and chalcopyrite (Richards, 1985).

The unaltered pyroxenite consists dominantly of clinopyroxene with lesser amounts of biotite and magnetite. Accessory minerals include apatite, monazite, zircon, zirkelite, ilmenite, pyrrhotite, pyrite and chalcopyrite (Richards, 1985).

The intrusion of carbonatite dykes introduced alkalis and other volatiles causing metasomatism of the pyroxenite. This metasomatism has produced the inner micaceous magnetite-amphibolite zone which has a major mineral assemblage of magnetite–phlogopite–carbonate–amphibole with the same accessory minerals as the pyroxenite zone plus pyrochlore, barite, bastnäsite, aeschynite, baddeleyite, pandaite and thornianite (Richards, 1985).

Lithologically the highest average rare earth and yttrium grades occur in the jasperoidal ironstone breccia. The carbonatite rocks have the highest average of rare earth concentrations and the biotite magnetite pyroxenite rocks have the highest average yttrium concentrations (Richards, 1985).

The following REE-bearing minerals have been identified from previous study (i.e., Sweetapple and Downes, 2010) divided by host rock type:

- **Original pyroxenite:** apatite, monazite
- **Metasomatised pyroxenite:** apatite, monazite, bastnasite
- **Carbonatite:** apatite (may locally be a major constituent), monazite, bastnasite, allanite

From the few samples lying in the oxidized zone, regolith lithologies are comprised of 50% or more monazite or apatite grains of varying size, cemented by one or more of apatite/collophane, (chalcedonic) quartz, goethite and fine Ca–Fe–P bearing mineral species. Apatite overgrowths, analogous to quartz overgrowths seen in quartz sandstones were documented in one sample. A comment made regarding an apatite-rich saprolite sample, indicated that apatite appeared to have formed in several episodes. There is also a suggestion of the presence of very fine secondary rare earth carbonates, tentatively identified as parisite ($Ca(Ce,La)_2(CO_3)_3F_2$) and synchysite ($Ca(Ce,La)(CO_3)_2F$) (Sweetapple and Downes, 2010).

5.4. HyLogging results

The database results and observation were applied to the Cummins Range CDD1 drill core.

5.4.1. CDD1 drill hole

The drill hole CDD1 is 402 metres long and it took two days to scan it with the HyLogger (Figure 9). It goes through both the mineralisation and regolith of Cummins Range intersecting jasperoidal ironstone breccia, carbonatite and pyroxenite.

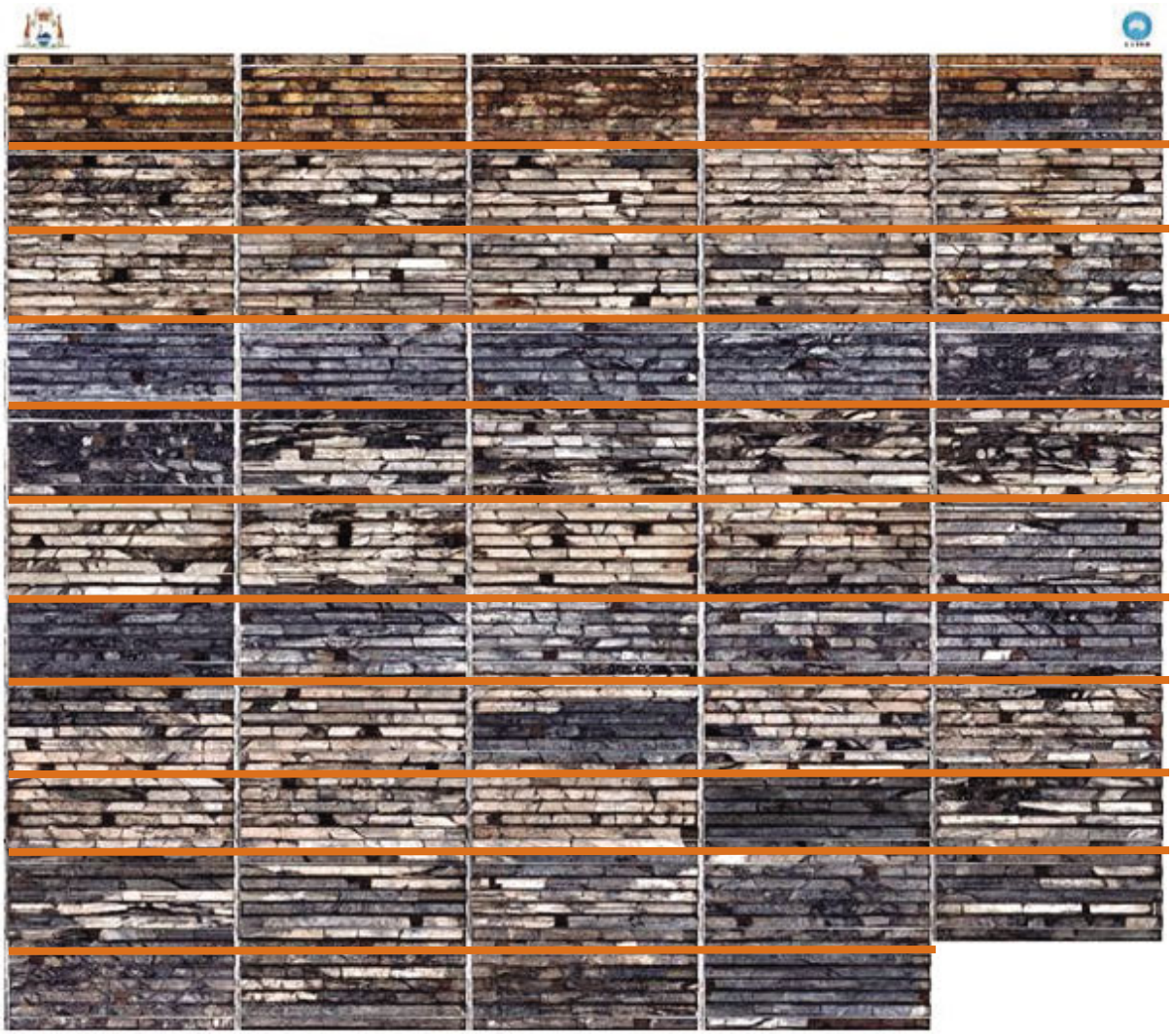

Figure 9 Image mosaic of the drill hole CDD1 from Cummins Range. Image from the TSG after being scanned with the HyLogger

Core should be "read" as though it were a book, that is, from top-left through to bottom-right within each core tray, and each tray is viewed in succession from top-left to bottom-right.

5.4.2. REE identification

Before any interpretation, it is essential to process the data with the TSG software consisting of cleaning the results, which involves five steps

1. The “Masking”, to mask out all the non-desired spectra (e.g., tray borders, wood blocks)
2. The “Depth Logging”, to put the right depth along the numerical core
3. The image creation to generate pictures of all trays and a composite mosaic from the high-definition camera of the HyLogger.
4. Trim spectral data using The Spectral Assistant (TSA).
5. Minerals or groups of minerals[1] that are not likely to be present (i.e., Selected in regards with the reports of Richards (1985) and Sweetapple and Downes (2010)) are switched off in the TSG database to avoid any misinterpretation when the drill cores spectra are compared to the database.

To detect REE within the cores “scalars[2]” had been created to search for the 580/745/800/870 nm features (Appendix 13). Those scalars were searching for one particular feature at the time (e.g., 745 nm) and by plotting several scalars at the same time, it was possible to locate the REE.

Features are found essentially in the jasperoidal ironstones (i.e., at a depth of 50 m to 100 m in the drill core) and sovite (i.e., 250–300 m) where assay results show the highest concentration in REE; no features at these wavelengths were found in the fresh pyroxenite (Appendix 12).

These feature are not as sharp as the one for the mineral database, it is because of that the core is a mixture containing only a percentage of the REE bearing minerals, however the features can still be recognized, particularly those at 745 nm and 800 nm. The 580nm and 870 nm features are not as sharp and can be easily missed in interpretation, but when they are present, they support the presence of REE.

[1] *Epidote, tourmaline, prehnite, pyrophyllite, garnets and all feldspars*

[2] *Threshold: 580nm=0.01 745nm=0.02 800nm=0.04 870nm=0.04*

6. Discussion

REE exploration is not well developed in nations outside China and has become lucrative to explore and to mine. There is a need for improving exploration techniques. Spectrometry is one of the advanced techniques available to geologists and the HyLogging system developed by the CSIRO is one way to apply it.

The database creation from scanning of museum specimens gave good results with the HyLogger. Signatures for REE could be readily found and features identified. These features seem to be related to particular elements within the mineral and with spectra from all the different elements it would be possible to determine which one contributes to each signature and features. Moreover, knowing what elements are present would be in the interest of geo-metallurgists.

Allanite did not give any result as the mineral is too dark to reflect light, it is important to notice that as some mineralisation or other minerals present in the drill cores or samples scanned might also have the same issue. A difference in spectra between phosphate, carbonate and xenotime was found and needs to be investigated.

By incorporating the database of scanned reference samples into the TSG library and after further studies, it could enable automatic recognition by the software when REE samples are scanned and interpreted.

The comparison with Cummins Range CDD1 drill hole showed that REE could be located within a core without particular preparation except cleaning. In addition, the HyLogger could be used for other drill cores. As the HyLogging technology is adapted in portable format (i.e., ASD™) and smaller format adapted for drill chips (i.e., HyChips™), application for absorption spectrometry to REE is promising.

The HyLogger being used during a drilling program could determine quickly and easily the rich REE zones on which to focus o further detailed study and analysis.

7. Recommendations

- The database of REE must be enlarged to improve the confidence in interpretation.
- Each rare earth element (as oxide) must be scanned with the HyLogger to know which elements contribute to the features and signatures.
- The database should be compared with different style of rare earth mineralisation including at different locations.
- The detection limits for REE through use of the HyLogger should be estimated.

8. Conclusion

The HyLogger can detect REE signature within minerals and cores. REE useful features are located in the VNIR, moreover the TIR present no interest as no features were found. Features diagnostic of REE exist in the SWIR, but are not so characteristic or sharp. In addition it is difficult to find diagnostic features in the SWIR because of the noise of the other minerals responding in that area. An absorption features shift is noted between REE bearing phosphate/carbonate. Additionally, xenotime can be readily and confidently identified by use of the HyLogger as it possesses a complete different signature.

By being a fast, non-destructive and informative technique the HyLogging™ system is helpful for REE exploration and mining companies.

References

Andrew, R.L.B., 1990. Cummins Range carbonatite, in: E., H.F. (Ed.), Geology of the Mineral Deposits of Australia and Papua New Guinea. The Australasian Institute of Mining and Metallurgy, Melbourne, pp. 711–713.

Bruker AXS, 2011. Working Principle – EDS system.

Chen, Z., 2011. Global rare earth resources and scenarios of future rare earth industry. Journal of Rare Earths 29, 1–6.

Christie, T., Brathwaite, B., Tulloch, A., 1998. Mineral commodities report 17 - rare earths and related elements. New Zealand Institute of Geological Nuclear Sciences Limited, p. 13.

Clark, R.N., 1999. Spectroscopy of rocks and minerals, and principles of spectroscopy in: Rencz, A.N., Ryerson, R.A. (Eds.), Manual of remote sensing. Wiley and Sons, Inc., New York, USA, pp. 3–58.

Cooper, W., 1990. Queensland mineral commodity report. Queensland Government Mining Journal, 383–389.

Dill, H.G., 2010. The "chessboard" classification scheme of mineral deposits: Mineralogy and geology from aluminum to zirconium. Earth-Science Reviews 100, 1–420.

Encyclopædia Britannica, 2011. Spectroscopy, in: Edition, E.B.O.A. (Ed.).

Fielding, D.C., Jaques, A.L., 1986. Geology, petrology and geochemistry of the Bow Hill lamprophyre dykes, Western Australia, Fourth International Kimberlite Conference. Geological Society of Australia Abstracts, Perth, pp. 24–26.

Hancock, E., Huntington, J., 2010a. The GSWA HyLogger TM : rapid spectral analysis and its application in detecting mineralization. Geological Survey of Western Australia, GSWA 2010 Extended Abstracts, Promoting the prospectivity of Western Australia.

Hancock, E., Huntington, J., 2010b. The GSWA NVCL Hylogger: rapid mineralogical analysis for characterizing mineral and petroleum core. Geological Survey of Western Australia, Record 2010/17, 21p.

Hoatson, D.M., Jaireth, S., Miezitis, Y., 2011. The major rare-earth-element deposits of Australia: geological setting, exploration, and ressources. Geoscience Australia, p. 204.

Humphries, M., 2010. Rare Earth Elements: the Global Supply Chain CRS Report For Congress, in: Service, C.R. (Ed.). U.S. Library of Congress.

Kanazawa, Y., Kamitani, M., 2006. Rare earth minerals and resources in the world. Journal of Alloys and Compounds 408–412, 1339–1343.

Kimberley Rare Earths, 2011. Quarterly Activities Report and Appendix 5B, Perth, p. 8.

Richards, M.N., 1985. Annual report for 1984 on exploration licence 80/113, Cummins Range, Mt. bannerman, SE 52–13, Western Australia. CRA Exploration pty Limited.

Rowan, L.C., Kingston, M.J., Crowley, J.K., 1986. Spectral reflectance of carbonatites and related alkalic igneous rocks; selected samples from four North American localities. Economic Geology and the Bulletin of the Society of Economic Geologists 81, 857–871.

Schweitzer, J., 2011. Scanning Electron Microscope. Purdue University.

Sweetapple, M., Downes, P., 2010. Petrographic and mineralogical studies of ten samples from the oxidised zone of the Cummins Range carbonatite, Western Australia. CSIRO, Perth.

U.S. Geological Survey, 2011. Rare Earths Statistics and Information.

Weidner, V.R., Barnes, P.Y., Eckerle, K.L., 1986. A Wavelength Standard for the Near Infrared Based on the Reflectance of Rare-Earth Oxides. National Bureau of Standards 91, 243–253.

Yeates, A.N., Muhling, P.C., 1977. Mount Bannerman, Western Australia-1:250 000 geological series. Bureau of Mineral Resources, Geology and Geophysics of Australia.

Appendixes

List of Appendixes

Allanite

MDC 4737
Mt Gratwick
W.A., Australia

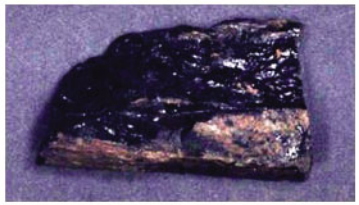

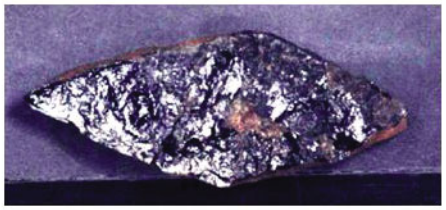

Appendix 1 Layout of allanite scanned with the HyLogger

Apatite

MDC 3828
Durango
Mexico

S 4665
Perth
Ontario, Canada

S 2024
South of the basin Melville
W.A., Australia

MDC 390
Quebec, Canada

S 2159
Wodgina
W.A., Australia

MDC 3576
Rum Jungle
N.T., Australia

Appendix 2 Layout of apatites scanned with the HyLogger

Bastnasite / Parasite

Bastnasite
S 1117
Itorendrika
Madagascar

Parasite
S 2845
Muzo bogata
Colombia

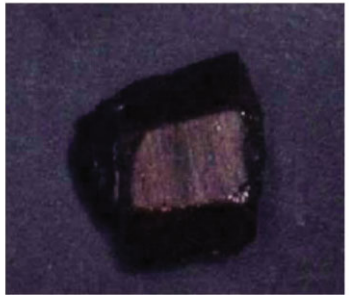

Appendix 3 Layout of bastnasite and parisite scanned with the HyLogger

Monazite

MDC 520
Rio Grande do Norte
Brazil

MDC 1464
Moolyella(N.W.)
W.A., Australia

S 2127
West Portland
Papireau Co,
Quebec, Canada

MDC 1276
Pilganoora (N.W.) 6 miles north
W.A., Australia

S 24
California Creek
Mt Garnet
QLD, Australia

S 1691
California Creek
Cook district
North QLD, Australia

MDC 2323
Carnarvon (N.W.) 100 miles
north
W.A., Australia

is actually a monazite

MDC 6324
Yinnietharra
W.A., Australia

Appendix 4 Layout of monazites scanned with the HyLogger

Xenotime

S3131
Yinnietharra district
W.A., Australia

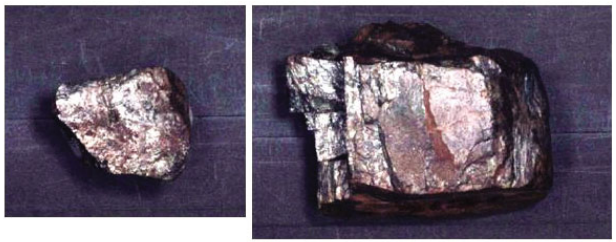

MDC 1180
Madagascar

MDC 1298
Hillside Homestead
W.A., Australia

Appendix 5 Layout of xenotimes scanned with the HyLogger

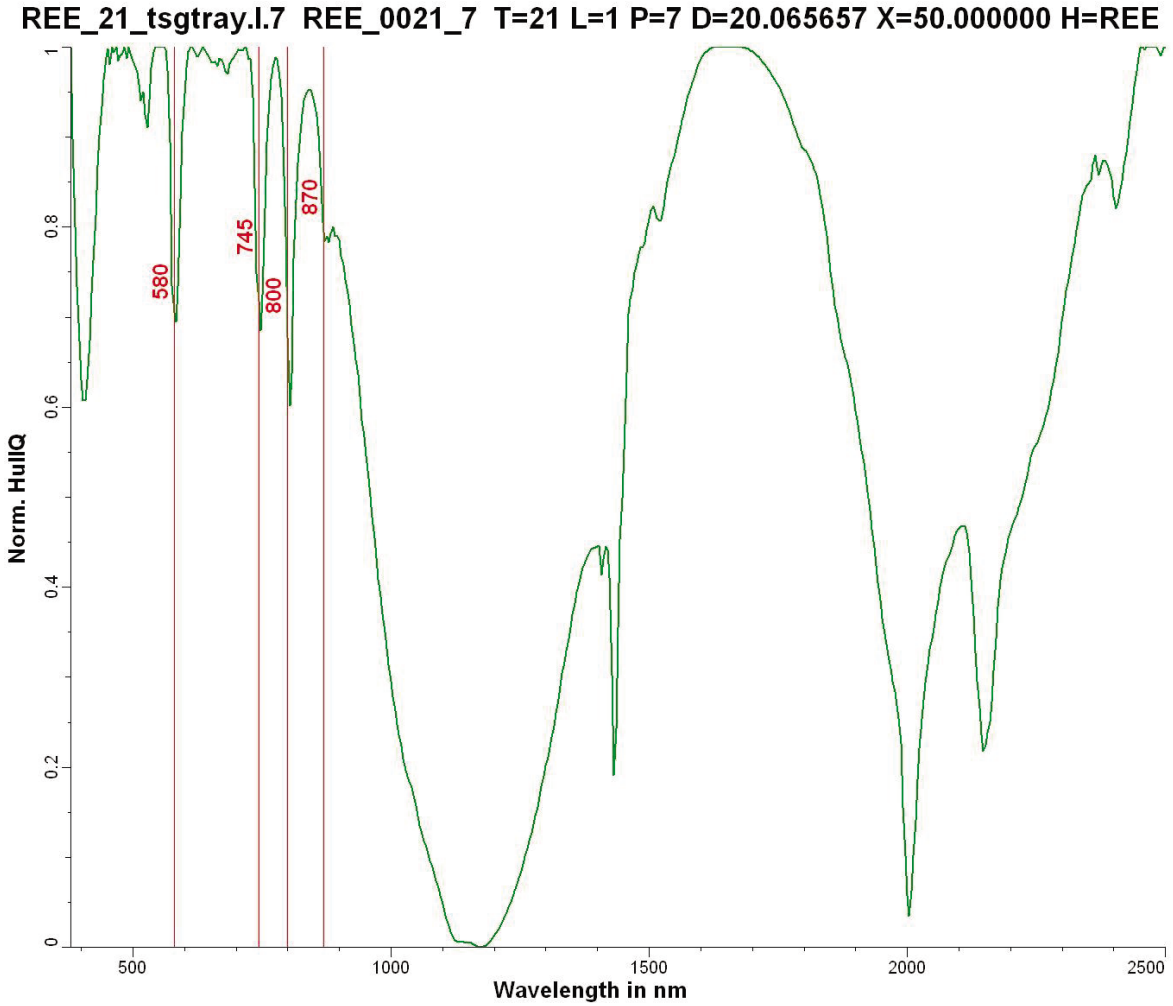

Appendix 6 Spectrum of apatite MDC 3576 with the REE features

10 MDC 1276 point 1			10 MDC 1276 point 2			10 MDC1276 point2a			11 MDC 6324			12 S 1691		
Element	***Wt %***	***Mol %***	***Element***	***Wt %***	***Mol %***	***Element***	***Wt %***	***Mol %***	***Element***	***Wt %***	***Mol %***	***Element***	***Wt %***	***Mol %***
Al2O3	3.34	6.31	Al2O3	30.83	26.06	Al2O3	35.78	25.51	Al2O3	2.07	3.67	Al2O3	0.63	1.29
SiO2	5.98	19.15	SiO2	38.91	55.8	SiO2	50.35	60.93	SiO2	5.28	15.93	SiO2	3.88	13.51
P2O5	28.18	38.22	P2O5	5.49	3.33	K2O	1.5	1.16	P2O5	30.45	38.86	P2O5	28.07	41.32
ThO2	2.2	1.61	K2O	1.03	0.94	TiO2	1.1	1	CaO	2.09	6.75	CaO	0.16	0.6
CaO	0.02	0.07	CaO	0.13	0.2	FeO	11.27	11.41	La2O3	9.16	5.09	La2O3	14.59	9.36
La2O3	5.57	3.29	TiO2	0.46	0.5	Total	100	100	Ce2O3	20.88	11.53	Ce2O3	32.78	20.87
Ce2O3	23.97	14.06	La2O3	1.6	0.42				Pr2O3	2.39	1.31	Pr2O3	3.47	2.2
Pr2O3	3.97	2.32	Ce2O3	6.3	1.65				Nd2O3	8.33	4.48	Nd2O3	11.04	6.85
Nd2O3	14.7	8.41	Pr2O3	1.03	0.27				Sm2O3	3.18	1.65	Sm2O3	0.68	0.41
Sm2O3	7.44	4.11	Nd2O3	3.63	0.93				Gd2O3	2.06	1.03	Gd2O3	0.52	0.3
Gd2O3	4.64	2.46	Sm2O3	1.72	0.43				ThO2	14.13	9.69	ThO2	4.16	3.29
Total	100	100	Gd2O3	1.21	0.29				Total	100	100	Total	100	100
			FeO	7.65	9.18									
			Total	100	100									

Appendix 7 EDAX results for monazites, part 1

13 S 24			14 MDC 1464			15 S 2127			16 MDC 520		
Element	***Wt %***	***Mol %***	***Element***	***Wt %***	***Mol %***	***Element***	***Wt %***	***Mol %***	***Element***	***Wt %***	***Mol %***
Al2O3	4.07	7.13	Al2O3	1.3	2.59	Al2O3	2.2	3.02	Al2O3	0.96	1.88
SiO2	7.04	20.95	SiO2	4.07	13.79	SiO2	10.9	25.33	SiO2	3.45	11.47
P2O5	22.63	28.49	P2O5	27.81	39.85	P2O5	20.04	19.7	P2O5	30.25	42.57
SO2	0.48	1.34	SO2	0	0	SO2	0.59	1.28	SO2	0.34	1.05
CaO	0.34	1.08	CaO	0.29	1.05	CaO	7.38	18.36	CaO	0.42	1.48
La2O3	11.13	6.1	La2O3	9.42	5.88	La2O3	4.19	1.79	La2O3	8.72	5.34
Ce2O3	25.32	13.79	Ce2O3	31.58	19.57	Ce2O3	8.84	3.76	Ce2O3	28.16	17.14
Pr2O3	2.82	1.53	Pr2O3	4.51	2.78	Pr2O3	1.24	0.53	Pr2O3	4.06	2.46
Nd2O3	8.5	4.51	Nd2O3	14.35	8.67	Nd2O3	3.93	1.63	Nd2O3	14.46	8.59
Sm2O3	0.55	0.28	Sm2O3	2.77	1.62	Sm2O3	0.39	0.16	Sm2O3	3.98	2.28
Gd2O3	0.38	0.19	Gd2O3	0.73	0.41	Gd2O3	0.63	0.24	Gd2O3	1.37	0.75
FeO	1.82	4.52	FeO	0.65	1.85	FeO	2.28	4.43	FeO	1.02	2.84
ThO2	14.93	10.1	ThO2	2.51	1.94	ThO2	37.39	19.77	ThO2	2.82	2.13
Total	100	100	Total	100	100	Total	100	100	Total	100	100

Appendix 8 EDAX results for monazites, part 2

8 S1117 bastnasite			9 S2845 parisite		
Element	**Wt %**	**Mol %**	**Element**	**Wt %**	**Mol %**
CaO	0.9	4.9	Y2O3	1.67	1.43
La2O3	36.8	34.41	UO2	0.76	0.54
Ce2O3	44.7	41.47	CaO	13.9	47.72
Pr2O3	4.13	3.81	La2O3	19.3	11.42
Nd2O3	9.53	8.63	Ce2O3	38.5	22.58
Sm2O3	0	0	Pr2O3	3.99	2.33
Gd2O3	0.34	0.29	Nd2O3	15.5	8.88
FeO	0.75	3.2	Sm2O3	1.13	0.63
ThO2	2.85	3.29	Gd2O3	1.62	0.86
Total	100	100	FeO	0.48	1.28
			ThO2	3.21	2.34
			Total	100	100

Appendix 9 EDAX results for bastnasite and parisite

5 MDC 1298			6 S 3131			7 MDC 1180		
Element	**Wt %**	**Mol %**	**Element**	**Wt %**	**Mol %**	**Element**	**Wt %**	**Mol %**
Al2O3	6.71	9.61	Al2O3	5.12	7.16	SiO2	7.02	19.04
SiO2	10.7	25.89	SiO2	10	23.8	P2O5	40.1	45.99
P2O5	36.5	37.5	P2O5	27.7	27.8	ThO2	5.33	3.29
Gd2O3	2.26	0.91	AgO0	2.86	3.79	Dy2O3	3.5	1.53
Dy2O3	3.92	1.53	CdO	1.85	2.06	Er2O3	2.53	1.08
Er2O3	2.25	0.86	CaO	0.52	1.33	Yb2O3	2.97	1.23
Yb2O3	2.38	0.88	TiO2	0.63	1.13	Y2O3	38.6	27.85
Y2O3	35.3	22.82	Gd2O3	1.24	0.49	Total	100	100
Total	100	100	FeO	2.18	4.33			
			Er2O3	1.87	0.7			
			Yb2O3	3.26	1.18			
			ThO2	8.28	4.47			
			Y2O3	34.5	21.77			
			Total	100	100			

Appendix 10 EDAX results for xenotimes

1 MDC 3576		1 MDC 3576 point2		2 MDC 3828		3 S2024		4 S4665 point 1		4 S4665 point 2		4 S4665 point 3	
Element	***Wt %***	***Element***	***Wt %***	***Element***	***Wt %***	***Element***	***Wt %***	***Element***	***Wt %***	***Element***	***Wt %***	***Element***	***Wt %***
P2O5	44.9	P2O5	42.6	P2O5	41.4	P2O5	43.3	P2O5	43.6	CaO	100	CaO	22.3
CaO	55.1	CaO	57.5	CaO	58.6	CaO	56.7	CaO	56.4	Total	100	La2O3	28
Total	100	Total	100	Total	100	Total	100	Total	100			Ce2O3	39
												Pr2O3	2.88
												Nd2O3	7.87
												Total	100

Appendix 11 EDAX results for apatites

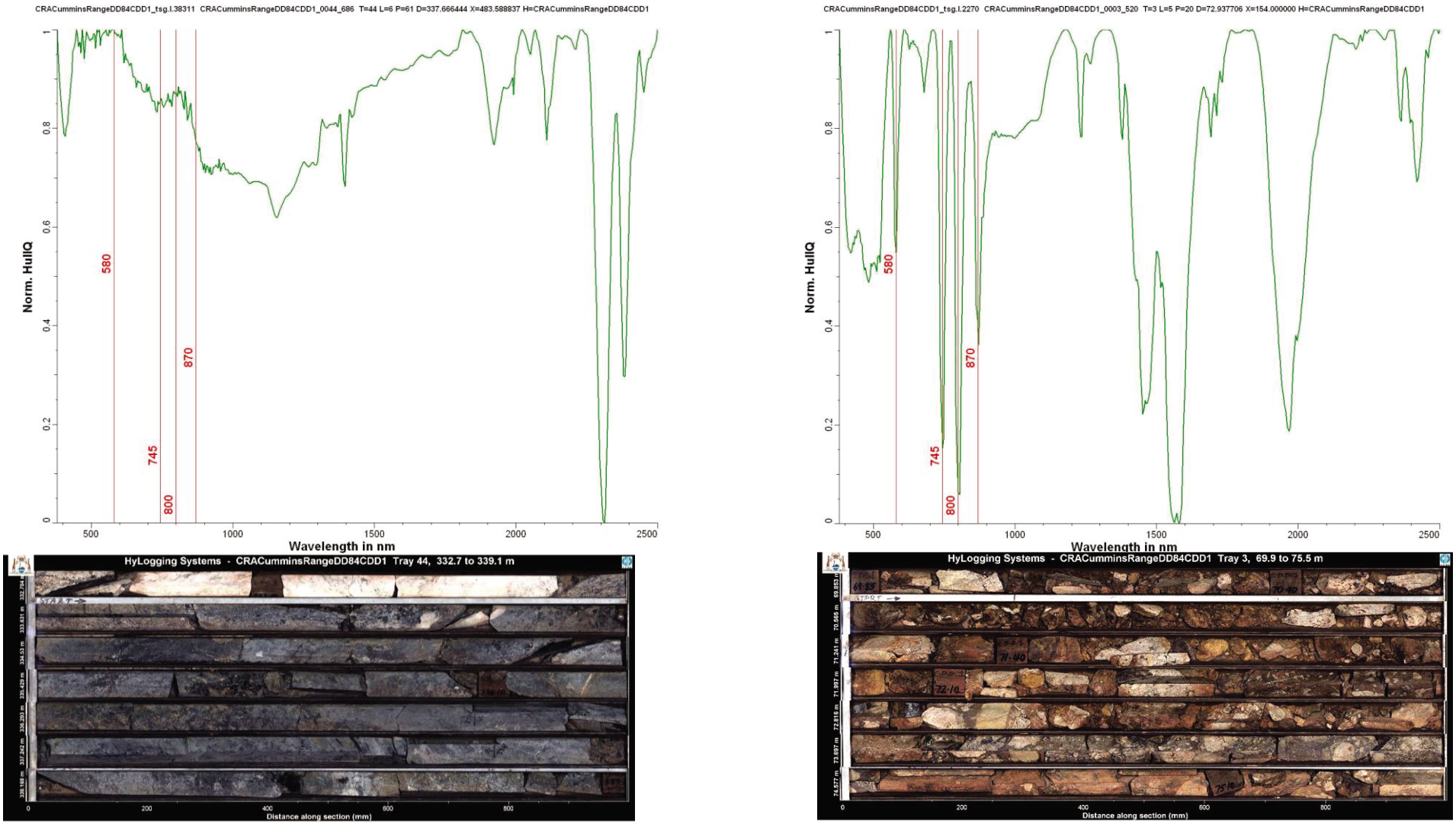

Appendix 12 Comaprison between spectrum without REE features and one with REE features. The first is located in the pyroxenite, whereas the second is located in the regolith profile

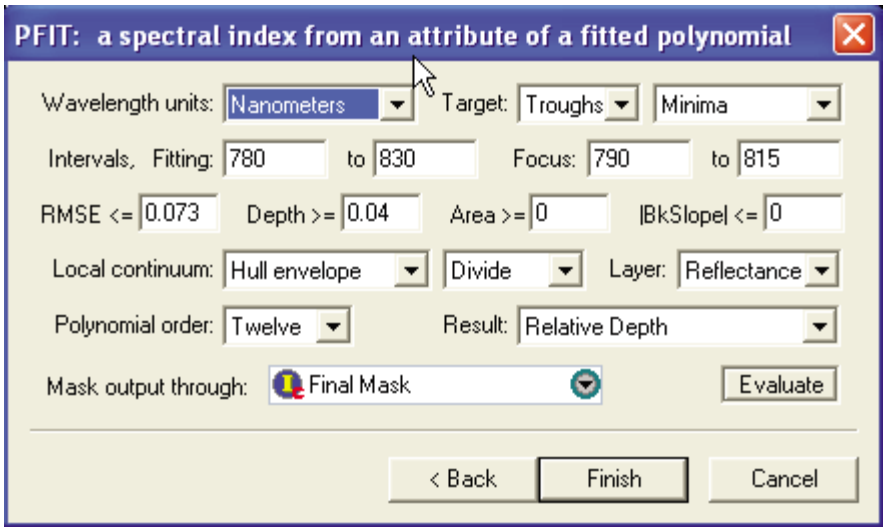

Appendix 13 Example of scalar created

VISIBLE ← → SWIR

Mineral	Absorption features in nanometre (nm)																									
Monazite				581			680	745	802	872							1090				1230					
Apatite	415			582				747	805	873																
Bastnasite	415			578			680	742	800	868	892						1086					1250				
Parisite				580			680	740	800	868	892						1094					1252				
Xenotime	412				652	668			809			915						1137				1255		1279	1304	
REE oxides																										
LREE																										
[1] Pr_2O_3				590						850		910														
[1] Nd_2O_3	420	475	525	580			680	740	800	870																
[1] Sm_2O_3	410	470											960				1090					1250				
HREE																										
[1] Eu_2O_3		470	530																							
[2] Dy_2O_3								743	799	886		907				1065	1096			1193	1230		1261			1321
[2] Ho_2O_3																		1132	1149							
[2] Er_2O_3													972	981	1013											

Continues below

SWIR →

Absorption features in nanometre (nm)																											Mineral
1374		1450								1550																	*Monazite*
																											Apatite
		1450								1540						1713											*Bastnasite*
		1459														1713											*Parisite*
	1410						1505								1701												*Xenotime*
																											REE oxides
																											LREE
		1460				1490				1560		1610												1980			[1] Pr_2O_3
	1420											1610				1710	1720										[1] Nd_2O_3
	1410									1550		1600															[1] Sm_2O_3
																											HREE
	1430																		1790	1850					2000	2008	[1] Eu_2O_3
												1612	1643	1682				1758									[2] Dy_2O_3
																				1847	1874	1886	1932	1971	2005		[2] Ho_2O_3
		1457	1462	1472	1478	1495	1504	1516	1536	1555	1577																[2] Er_2O_3

KEY: Non reliable | Doublet | Main features | Features | Weak

[1] REE oxides results from Weidner et al.(1986) [2] REE oxides results from Rowan et al.(1986)

Appendix 14 Full table of absorption features (VNIR and SWIR) (REE oxides from [2]Rowan et al., 1986; [1]Weidner et al., 1986)

RECORD 2012/12

HYPERSPECTRAL CHARACTERISATION OF RARE EARTH MINERALS

Morin Ka

This Record is published in digital format (PDF) and is available as a free download from the DMP website at <http://www.dmp.wa.gov.au/GSWApublications>.

Further details of geological products produced by the Geological Survey of Western Australia can be obtained by contacting:

Information Centre
Department of Mines and Petroleum
100 Plain Street
EAST PERTH WESTERN AUSTRALIA 6004
Phone: (08) 9222 3459 Fax: (08) 9222 3444
http://www.dmp.wa.gov.au/GSWApublications